Turk J Phys
35 (2011) , 265 – 272.

doi:10.3906/fiz-1103-9

Application of active-OSL Approximation to some experimental optical stimulated luminescence decay

Ayşe Güneş TANIR and Mustafa Hicabi BÖLÜKDEMİR
Faculty of Arts and Sciences, Gazi University, 06500 Ankara-TURKEY
e-mail: gunes@gazi.edu.tr

Received: 15.03.2011

Abstract

In this work, Active-OSL Approximation (AOSLA) suggested by our previous study was applied to experimental optical stimulated luminescence decay from some sediment samples. The explanation of the AOSLA was based on the radioactive decay law of successive disintegration. It allows obtaining the peak forms of luminescence mechanism. This work shows that detrapping constants that have great importance in dating and dosimeters studies can be rapidly and clearly found using the AOSLA. Also, it can be concluded that the OSL is a process similar to the radioactive decay law of successive disintegration.

Key Words: Optically stimulated luminescence decay, radioactive decay, kinetic parameters of OSL, deconvolution.

1. Introduction

The usual method of continuous-wave Optically stimulated luminescence (CW-OSL), uses constant excitation power. The observed OSL decay curve from such stimulation has an approximately exponential decay. Analysis of infrared stimulated luminescence (IRSL) decay from samples has been studied by many researchers [1–5]. In many works on CW-OSL, it has been shown that there are several overlapping OSL signals, each with different optical decay rates [6–8].

Bulur [9] introduced an alternative technique based on the linear increase of the stimulation light intensity (LMT) from zero to some maximum value. The measured OSL signal using LMT technique is in the peak form and the physical parameters of the traps have been obtained. Bulur [10] reported that LM-OSL of heated natural quartz can be well deconvoluted using a linear combination of several first-order peaks. There are several reports on the LM-OSL signals from quartz [11–15]. Kirsh and Chen [16] report a plot of $t \times I(t)$ as a function of $\ln(t)$ peak-shape curves (PS-plot) from which parameters were obtained.

This work presents the application of Active Optically Stimulated Luminescence Approximation (AOSLA) that has been suggested by us as a new view into the luminescence decay mechanism. AOSLA has been based on the decay of a radioactive nucleus and the details of it were given in our previous work [1]. The AOSLA

has been applied to experimental CW-IRSL decay curves from sediment samples named as Dağyaka and the experimental data by Liritzis and Bakopoulos [17], Bailey et al. [6] and Kuhns et al. [12] and tested that it can be successfully used to deconvolute the composite IRSL decay curves. The different traps contributing to the luminescence signal appear as different peaks in the AOSLA.

2. Simple description of the AOSL model

A short introduction to AOSLA was given in this section. See our study in [1] for a more extensive exposition.

The AOSL approximation is schematized in Figure 1, where all allowed transitions are indicated by arrows. The process is similar to the successive decay of a radioactive element but not identical. We have made the assumption that the absorption of energy from an ionizing radiation source by a sample causes the trapping states composed of shallow, medium and deep traps. We have also assumed that IR light stimulates the trapped electrons in shallow traps into the conduction band at rate λ_1, followed not only by recombination with trapped holes but also localization by medium or deep traps. Resultantly, the delocalized charges from deep traps go either to shallow traps or to the conduction band then back to recombination centers to produce the OSL.

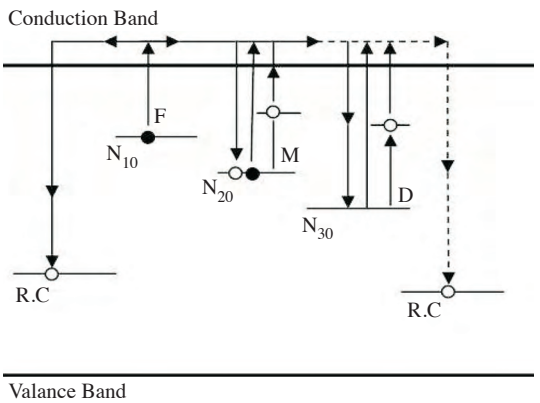

Figure 1. The schematic diagram of the proposed paths for movement of charges in samples during optical stimulation. Traps F, M and D are related to the fast, medium and slow components. The trapped electron concentrations are N_{10}, N_{20} and N_{30} at $t = 0$.

Accordingly, the Equations describing the IRSL counts and the activity (or OSL intensity) are proposed as follows:

$$N = N_1 + N_2 = N_{10}e^{-\lambda_1 t} + \frac{\lambda_1\lambda_2}{\lambda_2 - \lambda_1}N_{10}\left[e^{-\lambda_1 t} - e^{-\lambda_2 t}\right] + N_{20}e^{-\lambda_2 t} \tag{1}$$

$$I = I_1 + I_2 = \lambda_1 N_{10}e^{-\lambda_1 t} + \frac{\lambda_1\lambda_2}{\lambda_2 - \lambda_1}N_{10}\left[e^{-\lambda_1 t} - e^{-\lambda_2 t}\right] + N_{20}\lambda_2 e^{-\lambda_2 t}. \tag{2}$$

Equation (1) describes the luminescence photons counted experimentally over finite time intervals. N_1 is the number of atoms of parent element which decays λ_1 into its daughter element; and N_2 is the number of daughter element with λ_2, decay constant into a stable element having N_3 stable atoms. Assume that at time $t = 0$,

$N_1 = N_{10}$ and $N_2 = N_{20}$. While equation (1) has been used to plot the IRSL decay curves, equation (2) was found to be applicable to find the kinetic parameters of IRSL.

It is important to note here, for the compensation of theoretical and experimental data the term λ_2 should be inserted in the nominator of the second term in equation (1). This situation is different from radioactive decay law. Radioactive decay law of successive disintegration can be found in a book written by Krane [18].

In addition, the AOSL was applied to triple composite radioactive decay that $N_3 = N_{30}$ as $N_1 = N_{10}$, $N_2 = N_{20}$ at time $t = 0$. In this case, the equations describing the IRSL counts and the intensity are:

$$\begin{aligned} N &= N_{10}e\exp(-\lambda_1 t) + \frac{\lambda_1\lambda_2}{\lambda_2-\lambda_1}N_{10}\left[e^{-\lambda_1 t} - e^{-\lambda_2 t}\right] + N_{20}e^{-\lambda_2 t} \\ &+\frac{\lambda_2\lambda_3}{\lambda_3-\lambda_2}N_{20}\left[e^{-\lambda_2 t} - e^{-\lambda_3 t}\right] + N_{30}e^{-\lambda_3 t} \\ &+N_{10}\lambda_1\lambda_2\lambda_3\left[\frac{e^{-\lambda_1 t}}{(\lambda_2-\lambda_1)(\lambda_3-\lambda_1)} + \frac{e^{-\lambda_2 t}}{(\lambda_2-\lambda_1)(\lambda_2-\lambda_3)} + \frac{e^{-\lambda_3 t}}{(\lambda_3-\lambda_1)(\lambda_3-\lambda_2)}\right], \end{aligned} \tag{3}$$

$$\begin{aligned} I &= \lambda_1 N_{10}e^{-\lambda_1 t} + \frac{\lambda_1\lambda_2}{\lambda_2-\lambda_1}N_{10}\left[e^{-\lambda_1 t} - e^{-\lambda_2 t}\right] + \lambda_2 N_{20}e^{-\lambda_2 t} \\ &+\frac{\lambda_2\lambda_3}{\lambda_3-\lambda_2}N_{20}\left[e^{-\lambda_2 t} - e^{-\lambda_3 t}\right] + \lambda_3 N_{30}e^{-\lambda_3 t} \\ &+N_{10}\lambda_1\lambda_2\lambda_3\left[\frac{e^{-\lambda_1 t}}{(\lambda_2-\lambda_1)(\lambda_3-\lambda_1)} + \frac{e^{-\lambda_2 t}}{(\lambda_2-\lambda_1)(\lambda_2-\lambda_3)} + \frac{e^{-\lambda_3 t}}{(\lambda_3-\lambda_1)(\lambda_3-\lambda_2)}\right]. \end{aligned} \tag{4}$$

Equation (3) can be used to plot the IRSL decay curves that can be fitted to the sum of three simple exponential functions. PS-plot of decay curves have been achieved by using equation (4) for this situation.

3. Results and discussion

Here, the AOSLA was only applied to experimental OSL data obtained by us and by other experimenters. At first, the experimental IRSL signal from the Dağyaka sample exposed to 4 Gy β-doses was fitted to equation (1). The optical detrapping rates (or decay constants, λ_1 and λ_2) and trapping concentrations (N_{10} and N_{20}) were obtained and inserted in equation (2). A function $I(t) \times t$ versus ln t (PS-plot) was plotted using equation (2) for sample (and shown in Figure 2). This gives the peak-shaped presentation of IRSL decay curve analogous to the TL-like presentation used by Kirsh and Chen [16]. It can be possible to observe the two peaks of the PS curve become apparent at which correspond to the two optically sensitive electron traps. The decay-constants, λ_1 and λ_2, can be exactly found from Figure 2. Surely, equation (2) could be directly used to fit for experimental signal. The decay curve obtained from fitting to AOSL model was shown in the left-top of Figure 2. The fitted data is,

$$N(t) = 5217e^{-0.85t} + 1756e^{-0.1t} + \frac{5217 \times 0.85 \times 0.1}{(0.1-0.85)} \times (e^{-0.85t} - e^{-0.1t}).$$

The decay constants found from PS-plot are 0.5 and 0.1 s^{-1} respectively. While the deviation in λ_1 is large, it is zero for λ_2. As the difference decreases between the decay-constants, the deviation in λ_1 increases.

Luminescence mechanism for some limestone rock samples has been studied by Liritzis and Bakopoulos [17] and they have reported that their thermoluminescence (TL) signal can be expressed by a combination of one or two exponential components with some constant term. AOSLA model was applied to some of these samples named as LIG93-1, E93-1 and DEL5 by them. Figures 3–5 show the decay curves and PS-plots using the data from these samples in the work by them. It can be obviously seen that the peaks for these situations could be also displayed apparently.

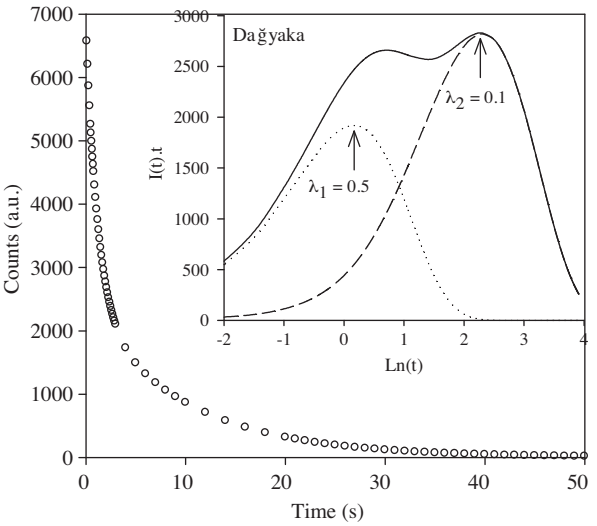

Figure 2. The application of the Active-OSL model for Dağyaka sample. As seen, the two decay constants appear as the noticeable peaks.

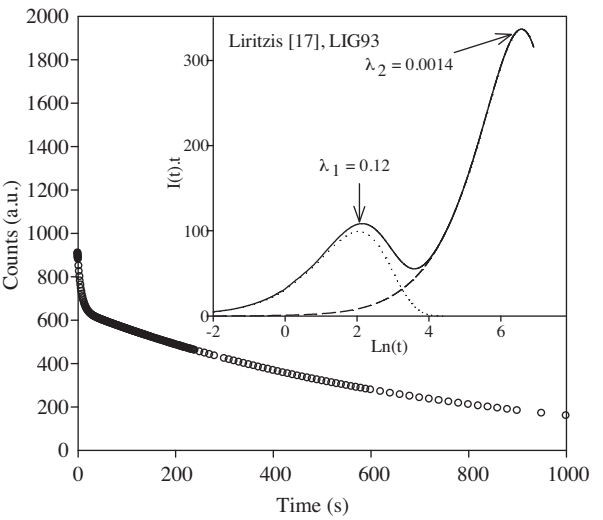

Figure 3. The data for the sample used here was taken from the work done by Liritzis and Bakopoulos [17]. The detail of the data was given in the text. The two peaks can be seen apparently.

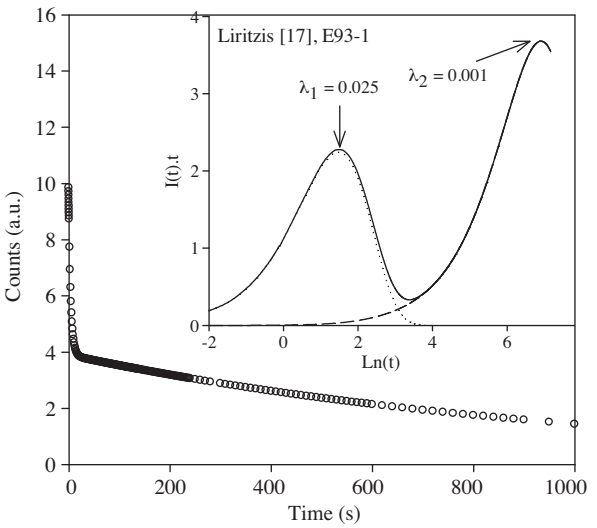

Figure 4. The sample named as E93-1 by Liritzis and Bakopoulos [17] was used to test the AOSL Approximation. The two peaks can be seen obviously and decay constants can be easily obtained from this figure.

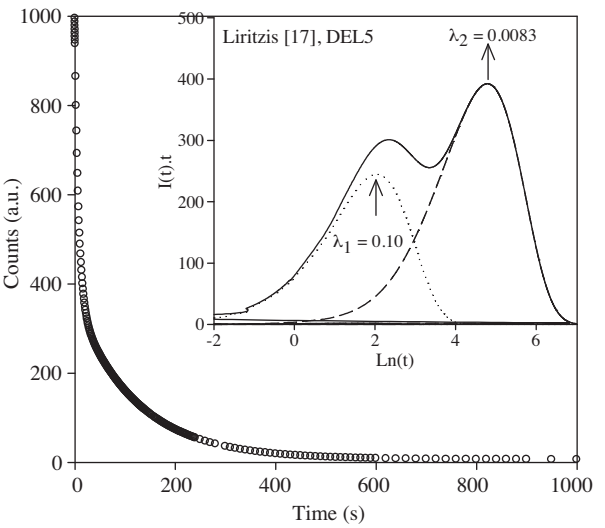

Figure 5. The application of AOSLA for the sample named as DEL5 by Liritzis and Bakopoulos [17].

The data from LIG93-1 (see Figure 3) sample is:

$$N(t) = 270e^{-0.13t}e^{+}642e^{-0.0014t} + \frac{270 \times 0.13 \times 0.0014}{(0.0014 - 0.13)} \times (e^{-0.13t} - e^{-0.0014t}).$$

The decay constants obtained by using AOSLA model are 0.12 and 0.0014 s^{-1}, respectively. The deviation is small (7 %) for λ_1 and zero for λ_2. The data from E93-1 sample is

$$N(t) = 611e^{-0.024t} + 387e^{-0.001t} + \frac{611 \times 0.024 \times 0.001}{(0.001 - 0.024)} \times \left[e^{-0.024t} - e^{-0.001t}\right]$$

and the obtained decay constants are 0.025 and 0.001 s^{-1}. The deviation in λ_1 is 4 % and zero for λ_2 (see Figure 4).

The third sample labeled DEL5 by Liritzis and Bakopoulos [17] was also considered to use in AOSLA model. Its luminescence data is

$$N(t) = 665e^{-0.13t} + 356e^{-0.0083t} + \frac{665 \times 0.13 \times 0.0083}{(0.0083 - 0.13)} \times \left[e^{-0.13t} - e^{0.0083t}\right]$$

and the obtained decay constants using their proposed model are: 0.1 and 0.0083 s^{-1}. As seen, the deviation is also negligible level (see Figure 5).

Deconvolution analysis using AOSLA model was applied to experimental CW-OSL curve from the sample used by Kuhns et al. [12]. They reported that the CW-OSL data from Canton dune sample (eolian sediment) can be described by the superposition of three first-order components. The work by Kuhns et al. [12] show the decay constants for fast, medium and slow components and the CW-OSL decay curve respectively. The luminescence data was approximately obtained from Figure 4 in the work by Kuhns et al. [12]. Inserting these data in Equation (3) and Equation (4), the OSL decay-curve and the PS-plot for the Canton dune sample were

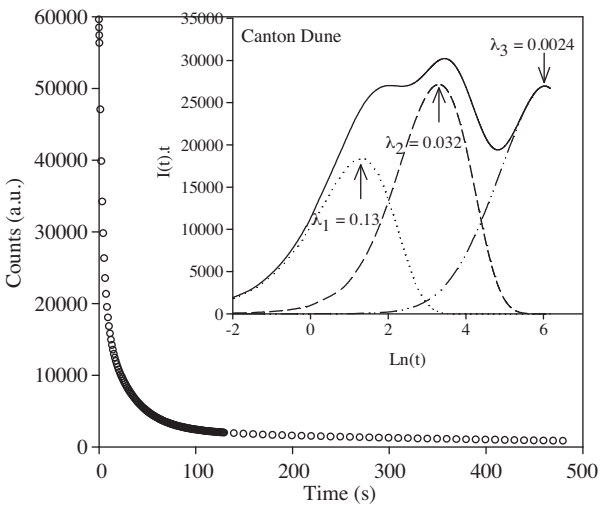

Figure 6. The data used here was taken from the work done by Kuhns et al. [12]. It has been named "Canton dune" by them. As seen, The AOSLA can give the three peaks correspond the three decay constants.

plotted and shown in Figure 6. The used data for the Canton Dune sample is:

$$N(t) = 5\times10^4 e^{-0.27t} + 16\times10^3 e^{-0.037t} + \frac{5\times10^4\times0.27\times0.037}{(0.037-0.27)}\times(e^{-0.27t}-e^{-0.037t})$$
$$+2250e^{-0.0024t} + \frac{16\times10^3\times0.037\times0.0024}{(0.0024-0.037)}\times(e^{-0.037t}-e^{-0.0024t}) + 5\times10^4\times0.27\times0.037\times0.0024$$
$$\times\left[\frac{e^{-0.27t}}{(0.037-0.27)(0.0024-0.27)} + \frac{e^{-0.037t}}{(0.037-0.27)(0.037-0.0024)} + \frac{e^{-0.0024t}}{(0.0024-0.27)(0.0024-0.037)}.\right]$$

For this sample, the three peaks correspond to three optically sensitive electron traps become apparent and the decay rates can be directly obtained from Figure 6. The significant increase in resolution of the peaks corresponding to luminescence detrapping constants can be provided using AOSLA model. The obtained decay constants using AOSL model (Figure 6) are 0.13, 0.032 and 0.0024 s^{-1}. Although the deviation in λ_1 is larger compared with other decay rates the three peaks can be seen obviously and λ_3 was accurately obtained. The reason of the large deviation in λ_1 is probably the fast bleaching. The first peak in PS-plot is bleached during 25 s.

Similar procedures were also applied to the experimental data reported by Bailey et al. [6]. The measured OSL signal from a natural Chaperon Rouge quartz sample (natural dose of about 12 Gy) held at 160 °C during measurements, and the half lives for the fast, medium and slow components are shown in Table 1, as reported by Bailey et al. [6]. The signal from the Chaperon Rouge sample has been shown by them to be the sum of three simple exponential components. The OSL intensities from fast, medium and slow components versus time have been shown in Figure 2 in their work. AOSLA model was applied to this data (Figure 7). For this sample, the first peak (fast component) does not become apparent. The reason of this situation may be the bleaching time and the small difference between the fast and medium decay constants. The fast component decays very rapidly and the time resolution is insufficient to obtain its decay constant.

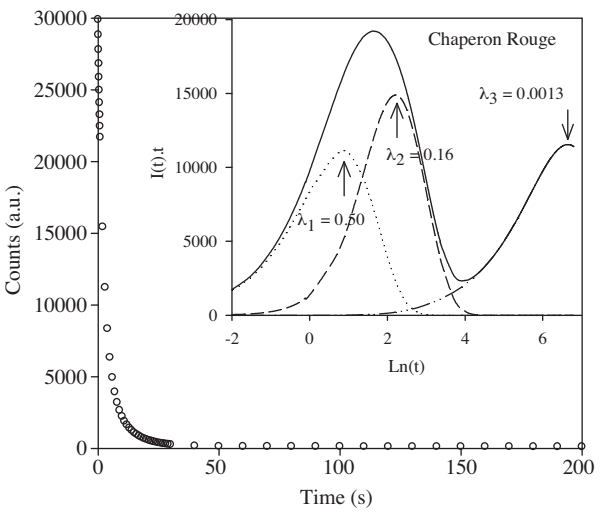

Figure 7. The application of Active-OSL Approximation for the sample named as Chaperon Rouge by Bailey et al. [6].

The data for this sample is:

$$N(t) = 3\times10^4 e^{-0.43t} + 900e^{-0.13t} + 90e^{-0.0013t} + \frac{3\times10^4\times0.43\times0.13}{(0.13-0.43)}\times\left(e^{-0.43t}-e^{-0.13t}\right)$$
$$+900\times\frac{0.13\times0.0013}{(0.0013-0.13)}\left(e^{-0.13t}-e^{-0.0013t}\right)+3\times10^4\times0.43\times0.13\times0.0013$$
$$\times\left(\frac{e^{-0.43t}}{(0.13-0.43)\times(0.0013-0.43)}+\frac{e^{-0.13t}}{(0.13-0.43)\times(0.13-0.0013)}+\frac{e^{-0.0013t}}{(0.0013-0.43)\times(0.0013-0.13)}\right).$$

The obtained decay rates using AOSLA model are 0.16 and 0.0013 s^{-1} for λ_2 and λ_3, respectively.

Thus, as the difference among λ_1, λ_2 and λ_3 increases, it becomes easier to separate individual luminescence components become easier since the possibility arises to resolve them as individual peaks. Furthermore, if necessary, the total contribution of components can be directly measured using the AOSLA model.

In the AOSL Approximation, detrapped charges can be retrapped in the same traps, or others. This only changes the trap concentration, i.e. it is not required to know the order of kinetic energy for the IRSL decay in AOSLA.

The decay constants of slow components can be exactly obtained using AOSL model. It is known that the slow components that characterize the deep traps are more stable than others and they have great importance in dosimeter and dating studies. Also the slow components should be assumed to be the dominate signals in the equivalent dose measurements.

It is important that, if there is a long tail in the experimental decay curve, the luminescence counts had to be measured for a long time with short space. It is enough that the experimental signal versus time should be only fitted to equation (3) or (4) to obtain the kinetic parameters of luminescence decay using AOSLA model. The residuals do not show any systematic trends for all the graphics.

Using AOSLA model it is possible to discriminate overlapping signals and to obtain the decay constants and trap concentrations. AOSLA allows clearly observing peak forms of the IRSL curves in the PS-presentation and the physical parameters of the decay can be quickly obtained. It provides a precise and an accurate determination of the OSL luminescence parameters. AOSLA is a practical way to obtain the kinetic parameters of OSL mechanisms.

It is not necessary to know the order of kinetics to use this model. The decay rates from each of trap types remain constant through the OSL measurements.

Acknowledgement

This work was supported by TUBİTAK grant number 106T478.

References

[1] G. Tanır, M. H. Bölükdemir, *Journal of Radioanalytical and Nuclear Chemistry*, **285**, (2010), 563.

[2] I. K. Bailiff and N. R. J. Poolton, *Nuclear Tracks and Radiation Measurements*, **18**, (1991), 11.

[3] I. K. Bailiff and S. M. Barnet, *Radiation Measurements*, **23**, (1994), 541.

[4] B. W. Smith, E. J. Rhodes, *Radiation Measurements*, **23**, (1994), 329.

[5] S. W. S. McKeever and R. Chen, *Radiation Measurements*, **27**, (1997), 525.

[6] R. M. Bailey, B. W. Smith, E. J. Rhodes, *Radiation Measurements*, **27**, (1997), 123.

[7] G. Adamiec, *Radiation Measurements*, **39**, (2005), 63.

[8] G. Kitis, I. Liritzis, A. Vafeiadou, *Journal of Radioanalytical and Nuclear Chemistry*, **254**, (2002), 143.

[9] E. Bulur, *Radiation Measurements*, **26**, (1996), 701.

[10] E. Bulur, *Radiation Measurements*, **32**, (2000), 141.

[11] N. L. Agersnap, E. Bulur, L. Bøtter-Jensen, S. W. S. McKeever, *Radiation Measurements*, **32**, (2000), 419.

[12] C. K. Kuhns, L. N. Agersnap, S. W. S. McKeever, *Radiation Measurements*, **32**, (2000), 413.

[13] M. Jain, A. S. Murray, L. Bøtter-Jensen, *Radiation Measurements*, **37**, (2003), 441.

[14] J. S. Singarayer, R. M. Bailey, *Radiation Measurements*, **37**, (2003), 451.

[15] J. S. Singarayer, R. M. Bailey, *Radiation Measurements*, **38**, (2004), 111.

[16] Y. Kirsh and R. Chen, *Nuclear Track Radiation Measurements*, **18**, (1991), 37.

[17] I. Liritzis, Y. Bakopoulos, *Nuclear Instruments and Methods in Physics Research B*, **132**, (1997), 87.

[18] K. S. Krane, Introductory Nuclear Physics, (John Wiley and Sons, NewYork, Chichester, Brisbane, Toronto, Singapore, 1988) p. 161.